Scientific Justification for the ALMA Compact Array (ACA)

Version October 7, 2001

1. Background

Ever since the conception of the large millimeter array project(s) in the 1980s, the problem of correctly imaging the large scale structure in maps of astronomical objects has been intensely discussed by the various science advisory groups. It is well known that an interferometer consisting of dishes of the same diameter (a so-called 'homogeneous array') is very good at high-resolution imaging of structures that are smaller than the primary beam. However, structures on larger scales are missed, even with multiple antenna pointings (a 'mosaic'), since the dishes cannot be placed together much closer than ∼1.2 times the dish diameter. Thus, the baselines that are correlated always have a minimum length which is somewhat larger than the dish diameter. For the 12-m ALMA antenna's, the minimum baseline length is about 15 m. This problem is therefore called that of the 'missing short spacings'. Recovering the large structures is important since they may contain a significant fraction of the flux and are therefore crucial for discussions of quantities such as the kinetic energy and momentum in gas motions.

The solution to this 'missing short spacings' problem is to add data from a large single-dish telescope and/or from an array of smaller dishes. Ideally, the diameter of the single-dish telescope should be twice as large as that of the interferometer dishes to pick up those structures on spatial scales that are missed by the interferometer. For ALMA, a compromise has been adopted in the baseline project, by using a few 12-m antenna's in single-dish mode (i.e., by not correlating their signals interferometrically) and adding the data to the interferometer data. Although this procedure can in principle produce very accurate images on large scales, even modest pointing errors can result in a considerable degradation of the dynamic range and fidelity of the maps (e.g., Cornwall 1988, A&A 202, 316). In particular, structures on intermediate scales of 6–15 m baselines may still be missed. As pointed out by Ekers (1999, AIP conf. series 180, 321), even though such errors can have only a small effect on the final maps, they result in a low-level background error over the whole image plane which can be significantly larger than the overall calibration error, especially for complex extended maps. Thus, such errors will make the ALMA goal of obtaining flux accuracies of 1–3% difficult to attain.

The ASAC and its predecessors have considered the option of a large >20-m single dish to complement ALMA, but rejected this possibility because of the difficulties in constructing a large telescope with sufficiently high surface and pointing accuracy needed for observations at high frequencies. The alternative option of an array of smaller dishes has therefore been adopted for ALMA as a possible enhancement in the 3-way project, and its performance has been intensely studied by the ALMA project, in collaboration with the ASAC. This array of smaller dishes, taken to be 12 dishes of 7-m diameter, is called the Atacama Compact Array (ACA). The motivation for the choice of number and size of the ACA dishes is given in ALMA memos 339 and 354. The plan is that the ACA will operate together with four 12-m antenna's in single-dish mode to recover the missing short spacings.

Simulations of the ACA (including calibration errors) have been performed by three independent groups (J. Pety, F. Gueth & S. Guilloteau at IRAM; K.-I. Morita at Nobeyama; M.A. Holdaway at NRAO) (see also the ASAC report and ALMA memos 354, 368, 374 and ***). The main conclusion is that the addition of the ACA to the baseline ALMA will improve the reliability

Table 1. Examples of ALMA programs with potential ACA candidates indicated

Distance	Object	Linear Size	Angular Size ($''$)	Sample ALMA projects	ACA?
$z \approx 5$	Proto galaxies	10 kpc	3	Blind survey of dust, CO, ...	$-$
$z \approx 0.5-??$	SZ effect	1 Mpc	200	Imaging of SZ effect to determine H_o	$+$
$z \approx 0.1-??$	Ultraluminous IR galaxies	10 kpc	6	Imaging structures, line ratios	$-$
$z \approx 0.01$	Galaxies at $z = 0.01$	10 kpc	50	Imaging structures, line ratios	$+$
10 Mpc	AGN tori	1 pc	0.02	Imaging of obscuring torus	$-$
10 Mpc	AGN, starburst centers	1 kpc	20	Structure and kinematics	$+$
10 Mpc	Nearby spirals	10 kpc	200	Imaging arm/interarm, line ratios	$+$
100 kpc	GMC in LMC/SMC	50 pc	100	Line ratios (CI/CO), structure	$+$
8 kpc	Galactic Center	5 pc	100	Mini spiral continuum, line	$+$
5 kpc	Hot cores, UC HII	0.05 pc	2	Line surveys, continuum	$-$
1 kpc	SNRs	0.05 pc	10	Continuum profile, line ratios	$-$
1 kpc	Late-type stars	0.02 pc	4	Line surveys, radial profile	$-$
0.1-1 kpc	Cluster-forming cloud cores	0.01-0.1 pc	2–100	Radial profile, polarimetry	$+$
0.1-1 kpc	Molecular outflows	0.01-0.5 pc	2–1000	Kinematics, cavities, line ratios	$+$
0.1 kpc	Infalling protostar envelope	5000 AU	50	Radial profile, line ratios	$+$
0.1 kpc	Protoplanetary disks	400 AU	4	Dust + molecules, gaps, line ratios	$-$
10 pc	Debris disks main-seq. stars	400 AU	40	Structure, gaps	$+$
	Planets		50	Structure atmosphere, e.g., Jupiter, Mars	$+$
	Comets		5	Jets, distributed molecules in coma	$-$
	Sun		1800	Limb brightening, solar activity	$+$

of the images and make the results less dependent on pointing and primary beam errors. The fidelity of the images —i.e., the inverse of the error— is improved by 30 to 100% by adding the ACA, reaching values of 30–60 under typical observing conditions, thereby allowing recovery of the smooth extended emission. These conclusions are based on a series of simulations, which were performed on a set of test images spanning a range in properties, including different spatial ranges, different intensity dynamic ranges, and various structures such as filaments or compact cores within an extended envelope. Another important result is that the addition of the ACA does not increase significantly the complexity of the data processing nor the required computing power. It does add some complexity in the operations, construction and maintenance of ALMA, since the ACA represents another array with a different type of antenna and more receivers, but efforts are made to duplicate as many elements as possible from the main array.

2. Science case

For the 12-m ALMA antenna's, the primary beam at the 'workhorse' 230 GHz frequency ($\sim$1 millimeter wavelength) is $22''$ (arcsec), whereas at the highest frequency of 900 GHz, it is only $6''$. Table 1 shows a list of high-priority ALMA science projects, with typical linear and angular sizes of the objects. The last column indicates those projects which are likely to benefit from the addition of the ACA data. The ACA is expected to play a particularly important role for projects at high frequencies, where the pointing errors on the 12-meter antenna's will be critical ($0.6''$ compared with a $6''$ beam) and where the objects will in general be larger than the primary beam. Typically, $\sim$25% of the projects (in time) are estimated to require the addition of ACA data. Because of its smaller collecting area, the ACA will need $\sim$4 times longer integration times than the main ALMA array to reach the required sensitivity. Thus, the ACA will be occupied close to 100% of its time with these projects.

In order to further justify the importance of the ACA, scientific analyses of the model results have been undertaken. This work is in progress and future studies will include a broader range in image properties. The advantages of adding the ACA depend on the source/image structure and content. The effects are often subtle, and may not be readily recognized by non-expert users. In the scientific

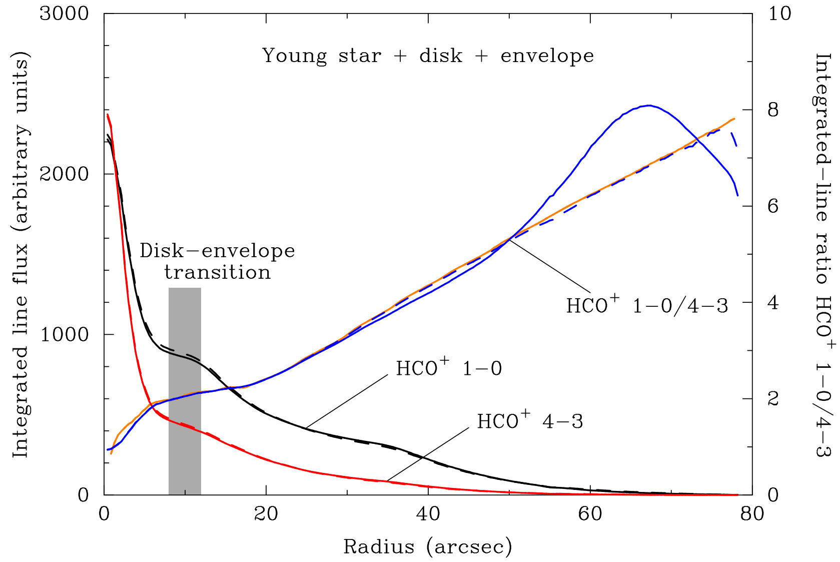

Figure 1. Radial intensity profiles of HCO^+ 1–0 and 4–3 emission in a model of an infalling and rotating envelope and disk around a low-mass protostar. The solid lines show the simulation results with data from ALMA and from 4 12-m telescopes operated in single-dish mode (ALMA + SD); the dashed lines include the ACA data (ALMA + SD + ACA). The right-hand axis shows the HCO^+ 1–0/4–3 line ratio, which is a measure of the density: the higher the ratio, the lower the density. The light (orange) line is the input model, the dashed line is the ALMA + SD + ACA result, whereas the dark solid line is the ALMA + SD result. The latter simulation shows significant deviations from the input model (M. Hogerheijde, priv. communication).

analysis performed so far, a few examples have demonstrated that, without the ACA, the images will miss key information leading to an inacurrate interpretation of the data. Two salient examples are given below.

Finally, it should be noted that the ACA can also serve as a stand-alone array in a compact configuration at any time for high frequency work. At 900 GHz, the ACA yields an angular resolution of 1.5″, similar to that provided by the compact configuration of ALMA at 230 GHz. Thus, maps of low- and high-excitation lines could be made with ALMA and the ACA, respectively, and compared on the same angular scale.

3. Two science examples

I. Structure of protostellar envelopes: In the deeply embedded phase of star formation, a protostar is surrounded by a circumstellar disk of size a few hundred AU (a few ″ at a distance of 100 pc) and a collapsing envelope of size a few thousand AU (up to 1′). The density structure of the envelope is a key parameter for testing different collapse models and needs to be recovered accurately by the array. Also, the amount of mass transferred from the cloud through the envelope to the disk and finally onto the growing protostar at each stage of evolution is an important question. Figure 1 shows a model of an extended infalling and rotating protostellar envelope for which radiative transfer calculations have been used to generate input images in the $J = 1 \rightarrow 0$ and $4 \rightarrow 3$ transitions of the HCO^+ molecule. The ratio of these transitions is sensitive to the density of the molecular gas and allows one to probe the density structure of the envelope. The simulation

Figure 2. Polarization maps of the Stokes I, Q and U parameters of the CO 230 GHz line toward Orion OMC1. The input model consists of actual data from the JCMT 15-m telescope combined with BIMA 6-m dish interferometer data (middle panels). Without the ACA (ALMA + single-dish only, bottom panels), the simulations completely fail to reproduce the input image, even for the Stokes I image, with fidelities of only 1–3. For the ALMA + single-dish + ACA simulations (top panels), the fidelities are improved to 10–20 and the structures are correctly reproduced (R. Crutcher, priv. communication).

results indicate that the density profile of the protostellar envelope can only be recovered properly when the ACA is included (Figure 1, right-hand axis). At approximately 2/3 of the radial extent, the error in the density determination amounts to about 30% when the short spacing information is lacking, leading to an incorrect determination of the radial density distribution. In addition, a qualitatively wrong conclusion that the envelope has an abrupt edge could be reached without the ACA. Adding the ACA, the error becomes significantly smaller, reaching 15% *** less?? *** at much larger radius, and the density distribution remains close to the input model. *** Michiel, do you agree with these statements?? ***

This test image is also characteristic of the Sunyaev-Zeldovich maps for distant galaxy clusters (see Figure x, refer to figure Carlstrom in Band 1 case), in the sense that there is a strong core surrounded by smooth extended emission. Thus, one can expect improvements by adding the ACA also for this important science case. *** is this indeed true? ***

II. Polarization: ALMA polarization studies will be able to map polarized emission in molecular clouds, supernova remnants, galaxies, and AGNs. For example, in molecular clouds, ALMA will measure magnetic field morphologies and strengths and be able to answer long-standing questions about the role of magnetic fields in the physics of interstellar turbulence, core formation and support, resolution of the angular momentum problem in star formation, and bipolar outflows. Polarization mapping is probably the most demanding of all ALMA instrumental requirements, for it needs precise measurements of polarized emission that is typically only a few % of the total emission in spite of the fact that instrumental polarization is of the same order.

One science case will be to measure the magnetic field in a turbulent molecular cloud in which cores and protoplanetary disks have formed. Angular scales will range from less than an arcsecond to many arcminutes. Missing polarized flux at zero and short interferometer spacings will lead to a complicated interplay between the partially resolved-out Stokes parameters from more extended structures and those from small-scale structures that will result in polarization maps that are qualitatively, and not just quantitatively, wrong. Indeed, tests made on polarization images of a case of a turbulent molecular cloud (Figure 2, total intensity I, and Stokes parameters Q and U) show that adding the ACA dramatically improves the recovery of the polarization information. Without the ACA, the fidelities are only 1–3 and the image is not reproduced even qualitatively. Errors on the position angle are of the order of 30°, making it nearly impossible to study the magnetic field morphology. Adding the ACA yields six times smaller errors, i.e. 5°, enabling to recover the polarization information and to study the ratio of turbulent to uniform magnetic field energies, an important parameter in star-formation theories. It is clear that without the ACA and single-antenna polarization data, ALMA's ability to address the crucial question of the origins of stars will be severely handicapped.